International Journal of Nanoelectronics and Materials
IJNeaM
ISSN 1985-5761 | E-ISSN 2232-1535

Numerical Analysis of the $ZnGeN_2$ Layer Effect on InGaN/GaN Multiple Quantum Well Light-Emitting Diodes

Laznek Samira 1[a]*, Messei Nadia 2[b], and Abdallah Attaf 3[b]

[a] *Department of SM, Faculty of Exact, Natural and Life Science, Mohamed Khider University, Biskra 07000, Algeria.*
[b] *Laboratory of Thin Films and Applications, Mohamed Khider University, Biskra 07000, Algeria.*
∗ Corresponding author. Tel.: +213-793-73-06-79; e-mail samira.laznek@univ-biskra.dz

Received 31 March 2023, Revised 27 July 2023, Accepted 17 August 2023

ABSTRACT

This paper discusses the effect of a $ZnGeN_2$ layer inserted into the wells of Type-I InGaN/GaN QWs LEDs on the electrical and optical properties by using the Silvaco TCAD Simulator. First, the new structure is compared to the standard type-I LED based on InGaN. We found that using $ZnGeN_2$ layer in the $In_{0.2}Ga_{0.8}N$-QWs LED leads to wavelength extending from the blue to the red region. Next, we highlighted the effect of quantum well number and In-molar fraction in the wells of $In_xGa_{1-x}N/ZnGeN_2$ type-II LEDs. As a result, increasing the number of wells from two to six QWs creates an extension of spontaneous emissions while keeping a low concentration of indium in the wells (x = 0.16) and improving the electrical and optical properties, as we found an improvement in light output power of 10.7% at $40Acm^{-2}$.

Keywords: *$ZnGeN_2$, band offset, Silvaco TCAD simulator, type- II, QWs*

1. INTRODUCTION

In recent years, white-colored light-emitting diodes (LEDs) have received a lot of attention due to their enormous potential for energy-saving in general lighting applications [1-3]. They have been generally fabricated by using InGaN /GaN quantum wells. GaN can exhibit emission over the full visible range due to wide energy band, which changes by adjusting the composition of the alloy [4, 5]. The use of high ln-content in InGaN/GaN LEDs QWs to broaden the emission band of the green and especially red wavelengths leads to large piezoelectric and spontaneous polarization fields that greatly affect efficiency reduction [6]. For this reason, several studies have proposed an effective solution to improve efficiency by using type-II InGaN/$ZnGeN_2$ in the active region of QWs LEDs.

A new promising semiconducting material with a large and direct gap has emerged as the zinc-germanium nitride $ZnGeN_2$. The high valence band offset forces holes to stay close together in the $ZnGeN_2$ layer. This lets the emission become wider in the red wavelength by using less In in the type-II lnGaN/$ZnGeN_2$ QWs structure [7, 8]. X-ray photoemission spectroscopy has been used in some studies to find that the valence band offset between $ZnGeN_2$ and GaN is 1.45–1.65 eV higher than that of GaN [9].

The zinc-germanium nitride $ZnGeN_2$ has characteristics similar to those of GaN where the lattice mismatch between them is less than 1%. The experimental lattice parameters for $ZnGeN_2$ are a = 3.1962 Å and c = 5.2162 Å, compared to those for GaN (a = 3.185 Å and c = 5.18 Å) [10]. In addition, the band gap of Zn-IV-N_2 materials covers a wide range of wavelengths ranging from infrared to ultraviolet, just like III-V materials, and is therefore remarkable for light-emitting devices [10]. The values for the spontaneous and piezoelectric polarizations also indicate that these materials will cause fewer problems than their III-V analogs, for example, the Stark effect [10].

Many search groups have studied the type-II QW structures to improve the optical and electrical properties of the InGaN/GaN QW structure. Among these type-II QW structures are the type-II InGaN/$ZnSnN_2$/GaN heterostructure and the type-II InGaN/GaNSb/GaN heterostructure [11, 12]. InGaN and $ZnGeN_2$ materials have structural and optical properties compatible with those of III-V elements [10]. Therefore, appear to be reasonable to realize the type-II InGaN/$ZnGeN_2$ heterostructure and to insert a thin layer of $ZnGeN_2$ into the active region of InGaN standard LEDs. On the other hand, the type -II InGaN/$ZnGaN_2$ /InGaN QW structure was proposed to obtain LEDs light emitting at longer wavelengths, typically beyond 530 nm with high efficiency while keeping a low concentration of indium in the wells.

In this work, we study the effect of quantum well number and the In-molar fraction on the electronic and optical properties of the type-II QWs LED structure combining InGaN and $ZnGeN_2$. To simulate the nanoscale effects in the QWs and their impact on device performance, we used SILVACO simulation software. SILVACO/TCAD uses the self-consistent 6-band Luttinger-Kohn k.p model to calculate band structures, which takes into account voltage effects, offsets of valence bands, and spontaneous and piezoelectric polarizations. Shockley–Read–Hall recombination and Auger non-radiative recombination mechanisms are also taken into account. Iteratively solving the Schrodinger and Poisson equations gives a description of the quantum of bound energy states in the quantum well with changing device bias and the use a free carrier model is to calculate spontaneous photon emission [13-17].

Nevertheless, the drift-diffusion model alone does not reflect the actual behavior of charge carriers in the quantum wells and barriers. Indeed, this model assumes that the bound carriers of the well are in equilibrium with the carriers of the bulk layers and make no difference between them [18]. For this reason, a new model was developed by SILVACO [18, 19]. The capture-escape model allows tracking the dynamics of bound carriers in quantum wells. It also allows for accounting for the effect of quantum charge by including it self-consistently in the Poisson equation.

2. DEVICE STRUCTURE

In this study, we used two device models with a rectangular chip size of 200x200 µm. One is a conventional LED emitting light blue, whose architecture is illustrated in figure 1a, and the second has the same structure, with layers of $ZnGeN_2$ 1 nm thick added inside the quantum wells as shown in figure 1b. This LEDs structure has a 200 nm thick p- GaN layer (Si: 10^{19} cm^{-3}), followed by an electron blocking layer (EBL) to reduce the electron-hole recombination at the p-side with AlGaN with 15% aluminum for a 45 nm thick (10^{19} cm^{-3}), active zone composed of 2 quantum wells of InGaN at 20% indium (3 nm thick), separated by undoped layers of 6 nm thick GaN barriers, and finally a 3µm thick n- GaN layer (Mg:10^{18} cm^{-3}). The $In_xGa_{1-x}N$ gap energy variation with fraction molar of indium and material parameters to be used for the proposed structure are shown in the two equations (1), (2) and in table 1.

The $In_xGa_{1-x}N$ energy gap was evaluated from GaN and InN Vegard's law:

$$E_g(In_xGa_{1-x}N)= xE_g(InN)+(1-x)E_g(GaN)-1.43x(1-x) \quad (1)$$

The Varshni law evaluated the variation of energy gap with temperature [20, 21]:

$$E_g(T)=E_g(0)-\delta T^2/\gamma+T \quad (2)$$

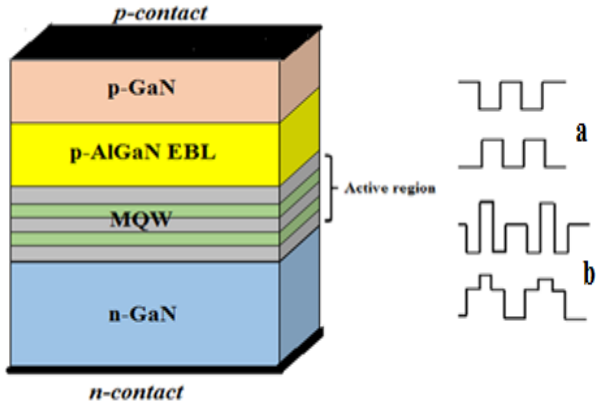

Figure 1. Schematic diagram of the LED structure investigated with 2-QW in the active region for (a) type-I GaN-InGaN-GaN and (b) type-II GaN-InGaN-$ZnGeN_2$-InGaN-GaN.

Table 1 Material parameters used in SILVACO at 300K [22, 23]

Material parameters	$In_{0.2}Ga_{0.8}N$	GaN	InN
$E_g(0)$ (eV)	2.64	3.42	0.7
γ(eV/k)	6.6 x10^{-4}	9.9 x10^{-4}	2.45 x10^{-4}
δ (k)	755	830	-
Hole lifetime τ_p (s)	10^{-9}	10^{-9}	-
Electron lifetime τ_n (s)	10^{-9}	10^{-9}	-
Electron Auger coefficient AUG_n (s)	10^{-34}	10^{-34}	-
Hole Auger coefficient AUG_p (s)	10^{-34}	10^{-34}	-
Radiative recombination rate constant COPT (s)	1.1 x10^{-8}	1.1 x10^{-8}	-
Electron Recombination Shockley-Read-Hall SRH. τ_n (s)	2x10^{-7}	2x10^{-7}	-
Hole Recombination Shockley-Read-Hall SRH.τ_p (s)	2x10^{-7}	2x10^{-7}	-

3. RESULTS AND DISCUSSION

3.1. Energy Band Alignment

Figure 2 shows potential energy profiles, where figure 2a is for the type-I GaN/$In_{0.2}Ga_{0.8}N$/GaN and figure 2b is for the type-II $In_{0.2}Ga_{0.8}N$/$ZnGeN_2$/ $In_{0.2}Ga_{0.8}N$ QWs LED structure at 40 A/cm^2. The wave functions of electrons (ψ_{e1}) and holes (ψ_{hh1}) in two quantum wells are also shown; 1e corresponds to the first conduction band excited levels and 1hh at valence band excited levels heavy holes. The well width of the type-I and type-II QWs structure is fixed as L_w =3 nm. The transitions between the 1e and 1hh energy levels E_{e1-hh1} are responsible for spontaneous emission peaks. Thus, the position of the spontaneous emission peak is entirely determined by the position of the 1e and 1hh energy levels and this explain the change in spontaneous emission peak when inserting the $ZnGeN_2$ layer as it will lead to a significant shift in the energy levels and a shift in the spontaneous emission of the LED. In addition, an overlap exists between the functions of electron and hole wave functions in the two wells, which will lead to an increase in radiative recombination, as shown in Figure 2c.

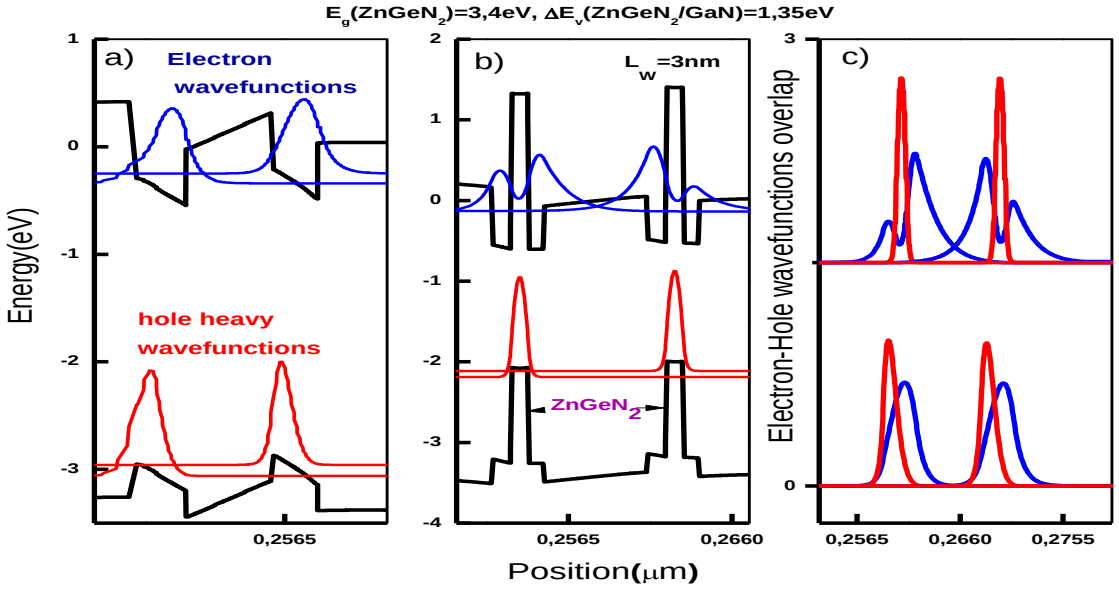

Figure 2. Potential energy profiles for (a) type-I GaN/$In_{0.2}Ga_{0.8}N$/GaN QWs, (b) type-II $In_{0.2}Ga_{0.8}N/ZnGeN_2$/ $In_{0.2}Ga_{0.8}N$ QWs at 40A/cm². ψ_{e1} and ψ_{hh1} are also shown as blue and red lines, respectively and figure (c) electron-hole wavefunctions overlap.

3.2. Comparison of Spontaneous Emission for the Conventional type-I and the type-II $In_{0.2}Ga_{0.8}N/ZnGeN_2$ /$In_{0.2}Ga_{0.8}N$ QWs LED structure.

Figure 3 compares the spontaneous emission of the conventional type-I GaN/$In_{0.2}Ga_{0.8}N$/GaN QWs with the type-II $In_{0.2}Ga_{0.8}N/ZnGeN_2$ /$In_{0.2}Ga_{0.8}N$ QWs LED structure according to various injection current densities of 10, 20 and 40A/cm². Figure 3 shows a significant enhancement of the spontaneous emission peaks of the type-II QWs compared to the conventional type-I QWs LED structure. As shown in Figure 3, the use of the $ZnGeN_2$ layer in the InGaN-QW extends the wavelength from the blue λ = 455 nm to the red region λ = 609 nm. The next step is modifying other parameters, such as the indium molar fraction and the quantum well number, and studying their effect on the optical and electrical properties to achieve the performance of these LEDs.

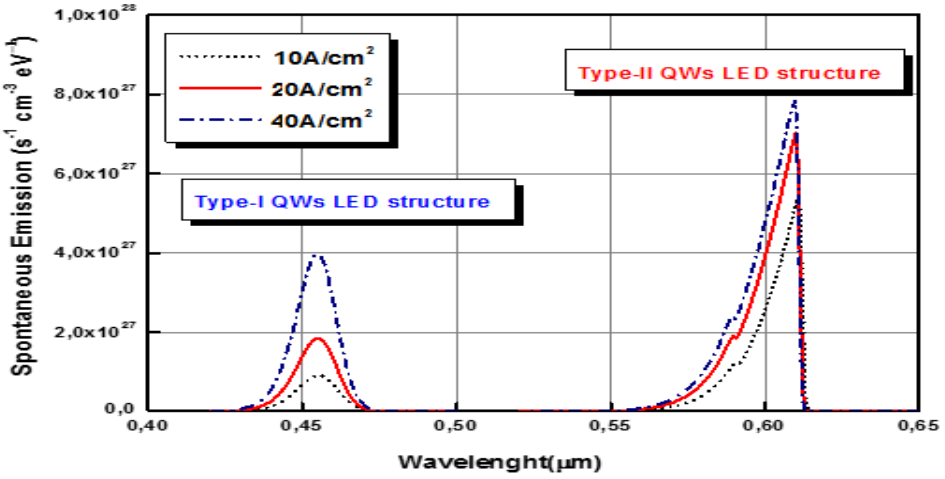

Figure 3. Spontaneous emission spectra on function of wavelength for type-I and type-II QWs LED structures at various injection current density.

3.3. Effect of Injection Current Density in the Spontaneous Emission of type-II $In_{0.2}Ga_{0.8}0N/ZnGeN_2$ QWs LED Structure.

We investigated the effect of injection current density in the spontaneous emission of the type-II $In_{0.2}Ga_{0.8}N/ZnGeN_2/In_{0.2}Ga_{0.8}N$ QWs LED structure. Figure 4 shows the effect of injection current density on conduction and valence bands. There is a negligible change in conduction and valence bands at current densities of 10, 20, and 40 A/cm², whereas, at 60, 80, and 100 A/cm² we observe a large change, which leads to a direct modification in energy levels, wavelengths, and spontaneous emission. Simulation results are shown in Table 2 and Figure 5.

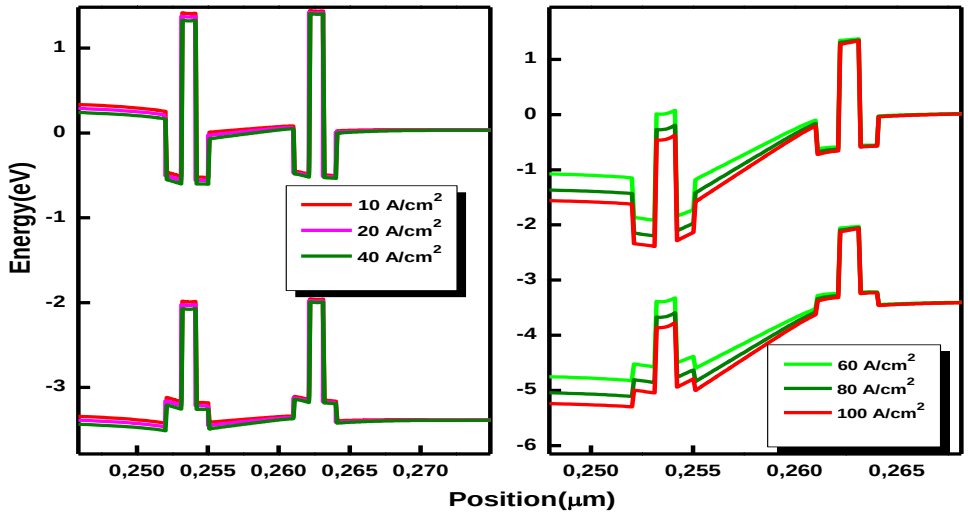

Figure 4. Potential energy profiles of the type-II $In_{0.2}Ga_{0.8}N/ZnGeN_2/ In_{0.2}Ga_{0.8}N$ QWs LED structure as a function of versus injection current density.

Table 2 Effect of injection current density in wavelengths and spontaneous emission of the type-II $In_{0.2}Ga_{0.8}N/ZnGeN_2/ In_{0.2}Ga_{0.8}N$ QWs LED structure.

Injection current (A/cm^2)	Peak energy (eV)	λ(nm)	Spontaneous emission (s^{-1} cm^{-3} eV^{-1})
10	2.032	610	5.30 x10^{27}
20	2.032	610	7.10 x10^{27}
40	2.032	611	7.86 x10^{27}
60	1.962	632	2.02 x10^{27}
80	1.937	640	2.21 x10^{27}
100	1.919	646	2.53 x10^{27}

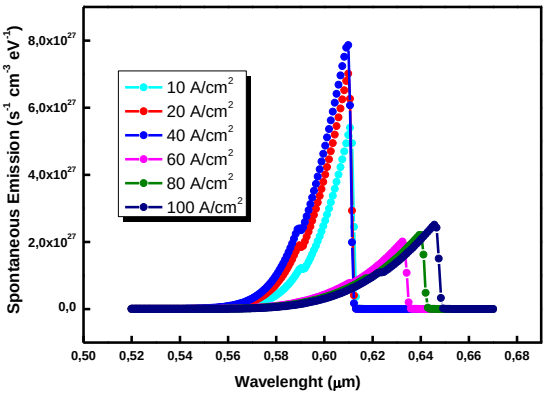

Figure 5. Spontaneous emission spectra of the type-II $In_{0.2}Ga_{0.8}N/ZnGeN_2/ In_{0.2}Ga_{0.8}N$ QWs LED structure as a function of versus injection current density.

Figure 6 shows peaks of spontaneous emission as a function of current density for type-II $In_xGa_{1-x}N/ZnGeN_2$ QWs structures with Indium content changed from x=0.16 to 0.20. Moreover, we observe that the type-II $In_xGa_{1-x}N/ZnGeN_2$ QWs structure has much larger spontaneous emission peaks for lower Indium content as a function of current density. On the other hand, the type-II $In_xGa_{1-x}N/ZnGeN_2$ QWs LED structure (x = 0.2) has smaller spontaneous emission peaks compared to the QWs structure with an Indium content equal to 0.16 and 0.18. The greatest value observed at 40 A cm^{-2} is 7.86 x10^{27} s^{-1} cm^{-3} eV^{-1}. After this value, a decrease is observed because the modification of the conduction and the valence band leads to a modification of the energy levels and a spontaneous emission. We conclude that the best spontaneous emission peak for QWs $In_xGa_{1-x}N/ZnGeN_2$ type-II structures is at indium content equal to x=0.16.

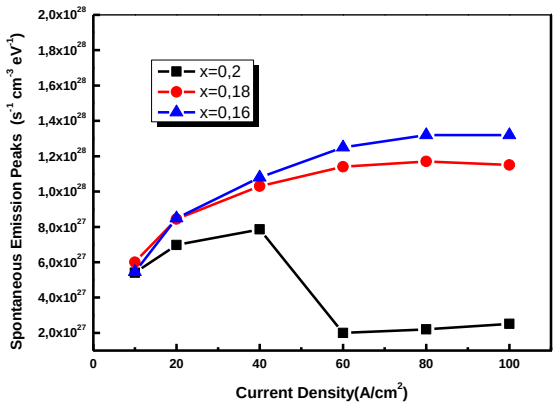

Figure 6. Peaks spontaneous emission of the type-II $In_xGa_{1-x}N/ZnGeN_2$ QWs LED structure as a function of current density with Indium content: x=0.16, 0.18 and 0.20

3.4. Effect of In-Molar Fraction (x) on the Electrical and Optical Characteristics of the type-II $In_xGa_{1-x}N/ZnGeN_2$/ $In_xGa_{1-x}N$ QWs LED structure.

The injection current density versus forward voltage of different In-molar fractions is simulated in both quantum wells layers as illustrated in figure 7. In the type-II InGaN/$ZnGeN_2$ QWs LED structure, the anode current decreases when the In-molar fraction increases in quantum wells. The best current density is of 115.98 A/cm² for x=0.16. There is a slight impact on EQE and light output power in the lower injection current, and under higher injection current density, the efficiency droop increases as the in-molar fraction in the two wells increases, as can be clearly seen in Figure 8a. At a density of constant current, it is a decreasing function of the increasing In-molar fraction. Therefore, at 40 A/cm², the luminous output powers of the structures are respectively equal to 15.46 mW, 15.16 mW, and 14.24 mW shown in figure 8b. As for spontaneous emission, we can see in figure 9, an increase in molar fraction in the two wells leads to a broadening of the wavelengths with a decrease in spontaneous emission peak.

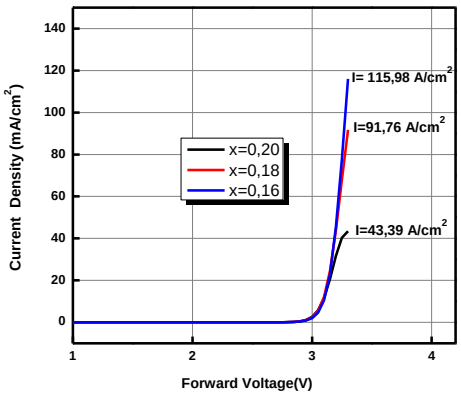

Figure 7. The injection current density versus forward voltage of the type-II $In_xGa_{1-x}N/ZnGeN_2$ QWs LED structure as a function for various molar fraction x.

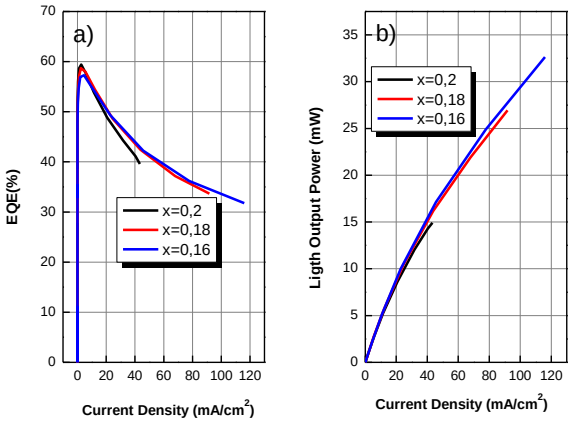

Figure 8. External quantum efficiency and Light Output Power of the type-II $In_xGa_{1-x}N/ZnGeN_2$ QWs LED structure as a function for various molar fraction x.

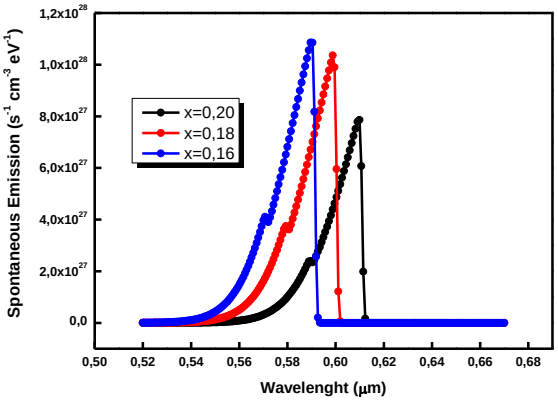

Figure 9. Spontaneous emission spectra of the type-II $In_xGa_{1-x}N/ZnGeN_2$ QWs LED structure as a function for various molar fraction x.

3.5. Effect of Quantum Well Number in the Optical and Electrical Characteristics of type-II $In_{0.16}Ga_{0.84}N$ /$ZnGeN_2$ QWs LED Structure.

The simulated concentration of electrons and holes in the active region of type-II $In_{0.16}Ga_{0.84}N/ZnGeN_2$ 2-4-6 QWs and the potential energy profile of the type-II 6-QWs structure of LED are shown in figures 10 a, b, and c, respectively, under an injection current density of 40 A/cm². When the QW number increases from 2 to 6, the results indicate that with a large number of quantum wells, the electrons and holes will be distributed more uniformly and will be more concentrated in the quantum wells, with different electron concentrations in each well, where we observe two very distinct peaks on either side of the $ZnGeN_2$ layer. Even the holes, their concentrations and distribution increases better in the $ZnGeN_2$ regions with the increasing quantum well number.

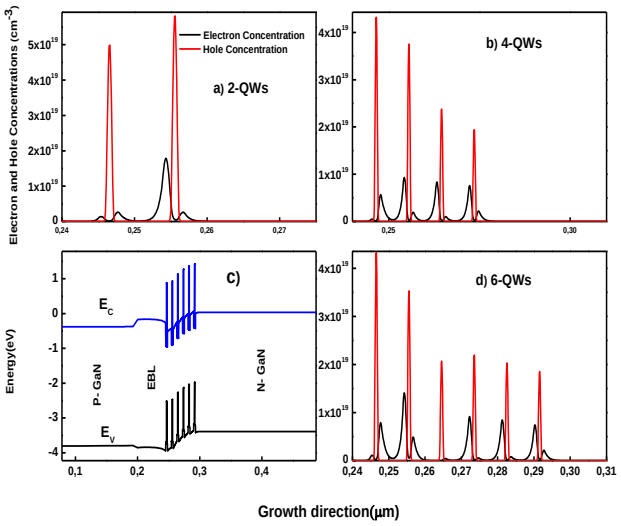

Figure 10. The concentration of electrons and holes in the active regions of type-II $In_{0.16}Ga_{0.84}N/ZnGeN_2$ QWs LED structure , (a) 2-QWs, (b) 4-QWs, (d) 6-QWs and (c) the potential energy profile of the type-II 6-QWs structure under injection current density 40 A/cm².

Figure 11 shows the injection current density versus forward voltage of the type-II $In_{0.16}Ga_{0.84}N/ZnGeN_2$ QWs LED structure with an increasing number of quantum wells simulated. The forward voltage at 40A/cm² decreases from 3.7 V to 3.19 as the quantum well number decreases from six to four and two, respectively.

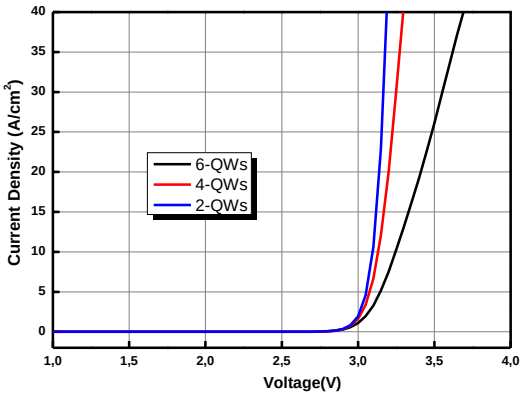

Figure 11. The Injection current density versus forward voltage of the type-II $In_{0.16}Ga_{0.84}N/ZnGeN_2$ QWs LED structure as a function for various number of QW.

To determine the effects of the quantum well number on the optical power and the efficiency, all parameters are kept constant, including the SRH lifetime as first step. Figure 12 shows the computed EQE and light output power with increasing current density for the LEDs with varying QW numbers. The simulated optical output power from the LEDs with 2, 4 and 6 QWs was measured, as presented in figure 12.b. It shows that the output power of 2, 4 and 6-QWs LEDs is 15.46, 16.86 and 17.30 mW, respectively, at the current density of 40 A/cm². The numerical optical output power is increased by 10.70% when the QW number increases from 2 to 6.

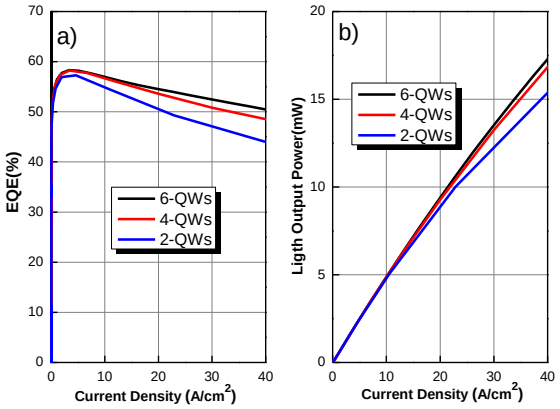

Figure 12. External quantum efficiency and Light Output Power of the type-II $In_{0.16}Ga_{0.84}N/ZnGeN_2$ QWs LED structure as a function for various number of QW.

When the QW number increases, we can see in figure 12 a. b the enhancement in the light output power and EQE at all current density levels, and this enhancement becomes increasingly apparent under higher injection current density. On the other hand, the efficiency loss (droop) reduces with increasing the number of QW. To explain this change on the EQE, radiative recombination rates are calculated (SRH and Auger) at 40 A/cm² and depicted in figure 13 a, 13 b and 13 c. All rates are distributed more significantly in the LED 2-QWs structure; the concentration of these rates is higher in the second well and slightly lower in the first well. For the structure with four quantum wells, the rates of radiative recombination, SRH, and Auger shifts for the first two QWs and remain for the last two quantum wells.

As for the last structure, which consists of 6-QWs, the radiative recombination rate, SRH and Auger are equally distributed amongst the six wells, which can be clearly seen in figure 13 a b c. In the $ZnGeN_2$ layers, Auger and SRH recombination equals zero, for 2-4-6 QWs LEDs because of the absence of electron concentration, as shown in figures 13 a b c.

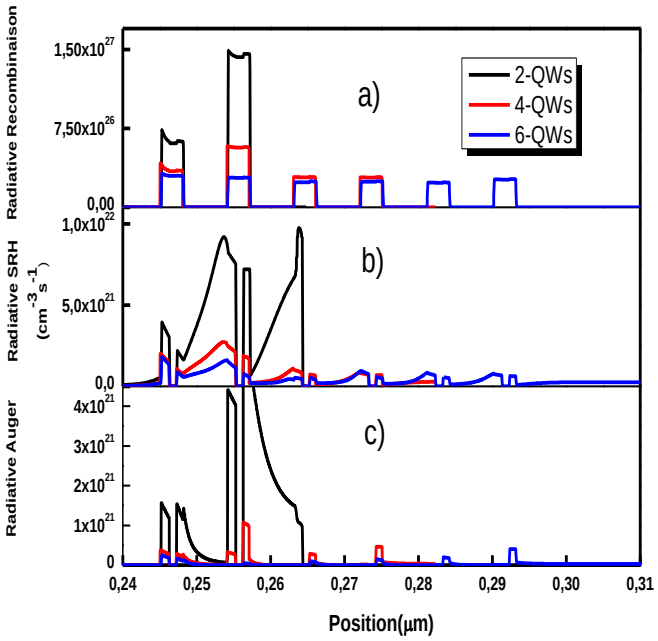

Figure 13. The rates of (a) radiative recombination, (b) SRH and (c) Auger at 40 A/cm² of the type-II $In_{0.16}Ga_{0.84}N$ /$ZnGeN_2$ QWs LED structure.

The type-II InGaN/$ZnGeN_2$ 2-QWs structure shows a significant efficiency loss compared to that for the type-II 4-QWs and the type-II 6-QWs structure at high-injected current densities. This efficiency droop is a result of a higher value of Auger recombination by electron-phonon coupling, as this phenomenon originates from the excitation of the Auger recombination and it have been demonstrated experimentally by J. Iveland et al [24-26].

Figure 14 and table 3 show the effect of increasing the number of wells in the active region on both the wavelength and the spontaneous emission. When increasing the number of wells, the wavelength extends from λ=589 nm to the λ=598 nm, this change is accompanied by a decrease in the spontaneous emission peak.

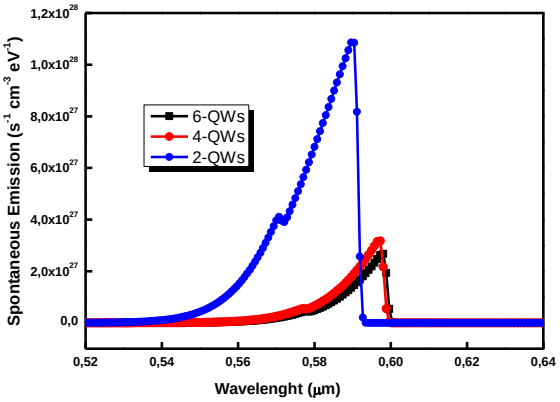

Figure 14. Spontaneous emission for the type-II $In_{0.16}Ga_{0.84}N$ /$ZnGeN_2$ QWs LED structure as a function for various number of QW.

Table 3 Effect number of quantum well in wavelengths and spontaneous emission for the type-II $In_{0.16}Ga_{0.84}N$ /$ZnGeN_2$ QWs LED structure.

Number of wells	Peak energy (eV)	λ(nm)	Spontaneous emission (s^{-1} cm^{-3} eV^{-1})
2-QWs	2.105	589	1.08 x10^{28}
4-QWs	2.080	596	3.21 x10^{27}
6-QWs	2.073	598	2.73 x10^{27}

4. CONCLUTION

The electronic and optical properties of type-II InGaN/$ZnGeN_2$-QWs LED structures have been investigated using the Silvaco TCAD simulator. The $ZnGeN_2$ layers inserted in InGaN/GaN QWs active region allow electron-hole wave function overlap by strongly confining the hole wave function in the $ZnGeN_2$ layers due to the large valence band offset. The conduction band offset between InGaN and $ZnGeN_2$ creates very distinct peaks on both sides of The $ZnGeN_2$ layer which affected the energy levels and overlap between electron-hole wave functions. As a result, the wavelength and the spontaneous emission peak intensity improve compared to the standard InGaN QWs LED. In this work, we have discussed the effect of the In-molar fraction in type-II $In_xGa_{1-x}N$/$ZnGeN_2$-QWs LED, where we have found a slight effect on the optical and electrical characteristics with an extension of the wavelength. Moreover, we have observed that the use of a high indium content (x = 0.2) in the type-II InGaN/$ZnGeN_2$-QWs LED structure for an injection current density greater than 40 A cm^{-2} leads to a modification of significant potential energy profile, which is reflected in both wavelengths and spontaneous emission, as it extends emission into regions with longer wavelengths. Finally, the use of MQWs of type-II InGaN/$ZnGeN_2$-QWs in LED devices is discussed. So, we propose this later as an effective way to increase the emission wavelength of the LEDs, keeping a low concentration of indium in the wells (x=0.16).

REFERENCES

[1] R. T. Velpula, B. Jain, H. Q. T. Bui, F. M. Shakiba, J. Jude, M. Tumuna, H. -D. Nguyen, T. R. Lenka, and H. P. T. Nguyen, "Improving carrier transport in AlGaN deep-ultraviolet light-emitting diodes using a strip-in-a-barrier structure," *Applied Optics*, vol. 59, no. 17, pp. 5272-5281, 2020.

[2] B. Jain, R. T. Velpula, H. Q. T. Bui, H.-D. Nguyen, T. R. Lenka, T. K. Nguyen, and H. P. T. Nguyen, "High performance electron blocking layer-free InGaN/GaN nanowire white-light-emitting diodes," *Optics Express*, vol. 28, no. 1, pp. 665-675, 2020.

[3] Y. Chen, C. Haller, W. Liu, S. Y. Karpov, J. -F. Carlin, and N. Grandjean, "GaN buffer growth temperature and efficiency of InGaN/GaN quantum wells: the critical role of nitrogen vacancies at the GaN surface," *Applied Physics Letters*, vol. 118, no. 11, p. 111102, 2021.

[4] T. Araki, Y. Saito, T. Yamaguchi, M. Kurouchi, Y. Nanishi, and H. Naoi, "Radio frequency-molecular beam epitaxial growth of InN epitaxial films on (0001) sapphire and their properties," *J. Vac. Sci. Technol. B*, vol. 22, no. 4, pp. 2139–2143, 2004.

[5] D. Brunner, H. Angerer, E. Bustarret, F. Freudenberg, R. Höpler, R. Dimitrov, R. Ambacher, and M. Stutzmann, "Optical constants of epitaxial AlGaN films and their temperature dependence," *Journal of Applied Physics*, vol. 82, no. 10, pp. 5090–5096, 1997.

[6] Q. Zhou, M. Xu, and H. Wang, "Internal quantum efficiency improvement of InGaN/GaN multiple quantum well green light-emitting diodes," *Journal Opto-Electronics Review*, vol. 24, no. 1, pp. 1–9, 2016.

[7] L. Han, K. Kash, and H. Zhao, "Designs of blue and green light-emitting diodes based on type-II InGaN-ZnGeN2 quantum wells," *Journal of Applied Physics*, vol. 120, no. 10, p. 103102, 2016.

[8] B. Hyot, M. Rollès, and P. Miska, "Design of Efficient Type-II ZnGeN2/In0.16Ga0.84N Quantum Well-

Based Red LEDs," *Rapid Research Letter*, vol. 13, no. 8, p. 1900170, 2019.

[9] M. R. Karim, B. Noesges, A. Jayatunga, B. H. D. Zhu, J. Hwang, W. R. Lambrecht, L. J. Brillson, K. Kash, and H. Zhao, "Experimental determination of the valence band offsets of ZnGeN2 and (ZnGe)0.94Ga0.12N2 with GaN," *J. Phys. D: Appl. Phys.*, vol. 54, no. 24, p. 245102, 2021.

[10] M. B. Tellekamp, M. K. Miller, A. D. Rice, and A. C. Tamboli, "Heteroepitaxial ZnGeN2 on AlN: Growth, Structure, and Optical Properties," *Cryst. Growth Des.*, vol. 22, no. 2, pp. 1270-1275, 2016.

[11] R. A. Arif, H. Zhoa, and N. Tansu, "Type-II InGaN-GaNAs quantum wells for lasers applications," *Applied Physics Letters*, vol. 92, no. 1, p. 011104, 2008.

[12] M. R. Karim and H. Zhao, "Design of InGaN-ZnSnN2 quantum wells for high-efficiency amber light emitting diodes," *Journal of Applied Physics*, vol. 124, no. 3, p. 034303, 2018.

[13] E. Kioupakis, Q. Yan, and C. G. Van de Walle, "Interplay of polarization fields and Auger recombination in the efficiency droop of nitride light-emitting diodes," *Applied Physics Letters*, vol. 101, no. 23, p. 231107, 2012.

[14] M. Filoche, M. Piccardo, Y. R. Wu, C. K. Li, C. Weisbuch, and S. Mayboroda, "Localization landscape theory of disorder in semiconductors. I. Theory and modeling," *Phys. Rev. B*, vol. 95, no. 14, p. 144204, 2017.

[15] C. K. Li, M. Piccardo, L. S. Lu, S. Mayboroda, L. Martinelli, J. Peretti, J. S. Speck, C. Weisbuch, M. Filoche, and Y. R. Wu, "Localization landscape theory of disorder in semiconductors. III. Application to carrier transport and recombination in light emitting diodes," *Phys. Rev. B*, vol. 95, no. 14, p. 144206, 2017.

[16] C. Mounir, U. T. Schwarz, I. L. Koslow, M. Kneissl, T. Wernicke, T. Schimpke, and M. Strassburg, "Impact of inhomogeneous broadening on optical polarization of high-inclination semipolar and nonpolar InxGa1−xN/GaN quantum wells," *Phys. Rev. B*, vol. 93, no. 23, p. 235314, 2016.

[17] M. Auf der Maur, B. Galler, I. Pietzonka, M. Strassburg, H. Lugauer, and A. D. Carlo, "Trap-assisted tunneling in InGaN/GaN single-quantum-well light-emitting diodes," *Appl. Phys. Lett.*, vol. 105, no. 13, p. 133504, 2014.

[18] SILVACO, *Atlas User's Manual*, Santa Carla, CA, USA, 2016, pp. 6-13.

[19] SILVACO, *ATLAS User's Manual, Device Simulation Software*, Santa Carla, CA, USA, 2015, pp. 6-254.

[20] P. G. Moses and C. G. Van de Walle, "Band bowing and band alignment in InGaN alloys," *Applied Physics Letters*, vol. 96, no. 2, p. 021908, 2010.

[21] J. R. Lang, N. G. Young, R. M. Farrell, Y.-R. Wu, and J. S. Speck, "Carrier escape mechanism dependence on barrier thickness and temperature in InGaN quantum well solar cells," *Applied Physics Letters*, vol. 101, no. 18, p. 181105, 2012.

[22] J. Wu, W. Walukiewicz, K. M. Yu, J. W. Ager III, E. E. Haller, L. Hai, and W. J. Schaff, "Small band gap bowing in InxGa1−xN alloys," *Applied Physics Letters*, vol. 80, no. 25, pp. 4741–4743, 2002.

[23] J. Wu and W. Walukiewicz, "Band gaps of InN and group III nitride alloys," *Superlattices and Microstructures*, vol. 34, no. 1-2, pp. 63-75, 2003.

[24] G. Verzellesi, D. Saguatti, M. Meneghini, F. Bertazzi, M. Goano, G. Meneghesso, and E. Zanoni, "Efficiency droop in InGaN/GaN blue light-emitting diodes: Physical mechanisms and remedies," *Journal of Applied Physics*, vol. 114, no. 7, p. 071101, 2013.

[25] J. Iveland, L. Martinelli, J. Peretti, J. S. Speck, and C. Weisbuch, "Direct Measurement of Auger Electrons Emitted from a Semiconductor Light-Emitting Diode under Electrical Injection: Identification of the Dominant Mechanism for Efficiency Droop," *Phys. Rev. Lett.*, vol. 110, no. 17, p. 177406, 2013.

[26] E. Kioupakis, P. Rinke, K. T. Delaney, and C. G. Van de Walle, "Indirect Auger recombination as a cause of efficiency droop in nitride light-emitting diodes," *Applied Physics Letters*, vol. 98, no. 16, p. 161107, 2011.